Available online at www.eccomasproceedia.org
Eccomas Proceedia COMPDYN (2021) 1574-1582

ECCOMAS
Proceedia

COMPDYN 2021
8th ECCOMAS Thematic Conference on
Computational Methods in Structural Dynamics and Earthquake Engineering
M. Papadrakakis, M. Fragiadakis (eds.)
Streamed from Athens, Greece, 28 - 30 June 2021

REDUCTION OF LOCAL DAMAGES IN PRECAST POST-TENSIONED SEGMENTAL BRIDGE PIERS

Parya Ahmadi[1], Ehsan Ahmadi[2], and Mohammad M. Kashani[3]

[1] MSc, University of Mohaghegh Ardabili, Ardabil, Iran
Ahmadii.Parya@gmail.com

[2] Lecturer, Birmingham City University, Birmingham, UK
Ehsan.Ahmadi@bcu.ac.uk

[3] Associate Professor, University of Southampton, Southampton, UK
Mehdi.Kashani@soton.ac.uk

Abstract

The application of precast post-tensioned segmental (PPS) bridge piers is growing in order to reduce global damages through rocking motion of the segments when subject to lateral excitations. However, local damages still exist in form of concrete spalling and crushing at the compression zones when one segment rocks on top of the underlying segment. Hence, this work will address reduction of these local damages in PPS piers through confinement of concrete segments by glass-fibre reinforced polymer (GFRP) tubes and use of elastic layers between segments at the joints. To achieve this goal, a robust Finite Element (FE) model is first developed in ABAQUS software, and is experimentally validated using the existing literature. The cyclic behaviour of the experimentally-validated FE model is then determined. It was found that the GFRP tubes and elastic layers significantly reduce local damages of PPS piers at the joints.

Keywords: Precast Post-Tensioned Segmental Piers, Glass-Fibre Reinforced Polymer, Finite Element Model, Elastic Layer, Cyclic Loading.

1 INTRODUCTION

Bridges are one of the crucial components of any transport network and any small disruption in their functionality can result in enormous economic damages and life losses. In particular, lateral excitations such as earthquake, can cause severe damages in bridge structures. Conventional cast-in-place (CIP) reinforced concrete (RC) piers are constructed monolithically with the bridge deck, and experience permanent damages in form of plastic hinges during

ISSN:2623-3347
Peer-review under responsibility of the organizing committee of COMPDYN 2021.
doi:10.7712/120121.8582.18523

severe earthquake loadings. One of the most effective solutions to avoid any plastic hinge, widely considered by researchers in accelerated bridge construction (ABC) [1], is precast post-tensioned segmental (PPS) piers [2]. In ABC, the concrete segments are manufactured offsite with higher quality, and then transferred to the construction site to be assembled. Additionally, the construction process is expedited, and environmental pollution is reduced. The rocking mechanism of the segments and self-centering effect of the post-tensioned tendon decrease the residual deformation of the PPS piers [3].

On the other hand, application of fibre reinforced polymer (FRP) material is growing in concrete piers due to its high stiffness and resistance against corrosion, weathering, and chemical attacks [4,5]. Using FRP around concrete piers enhances their performance by adding extra confinement to the concrete. In existing piers, FRP tubes are used to strengthen the pier, and in design of new piers, FRP tubes increase axial loading capacity of the pier [4]. FRP tubes also prevent the cover concrete from spalling, and significantly increase the ductility and lateral strength of the pier subject to seismic loading events [6].The FRP tubes have larger flexural strength and higher strength-to-weight ratio compared to steel tubes, and reduce the creep strain of the confined concrete [7,8].

In moderate- and high-seismicity regions, each segment of the PPS piers may still experience local damages at the contact interfaces (e.g. compression zones at the joints) in form of concrete spalling and crushing [4]. This is because of high stress concentration at the joints due to high compressive stresses [9]. To reduce or even eliminate concrete spalling and crushing at the joints, the segments were confined with steel jackets [10,11,12]. However, the steel jackets yield, and thus induce permanent residual deformations in the pier. Therefore, this study adopts a new approach in order to reduce the local damages and a damage-free PPS pier. The current study numerically investigates PPS piers confined with glass fibre reinforced polymer (GFRP) tubes, where elastic layers are used between the segments. To achieve this aim, a robust FE model is first developed and validated. Then, cyclic behavior of the pier is studied to investigate the effects of GFRP tubes around the segments and elastic layers between the segments.

2 NUMERICAL MODELLING

Four PPS specimens are modelled: (1) PPS pier without GFRP tube and elastic layer, P, (2) PPS pier with GFRP tubes, PT, (3) PPS pier with elastic layers, PL, and (4) PPS pier with GFRP tubes and elastic layers, PTL. To study the effects of the flexibility of the elastic layers between the segments, three values of Young's modulus are considered for the elastic layers: 05, 10 and 15 GPa. All the PPS specimens are summarized in Table1, and the FE models of the PPS piers are shown in Figure 1.

Pier Name	Pier Description	GFRP Tube	Elastic Layer (E_{layer})
P	Without GFRP tube and elastic layer	-	-
PT	With GFRP tubes	✓	-
PL05	With elastic layers	-	✓ (05 GPa)
PL10		-	✓ (10 GPa)
PL15		-	✓ (15 GPa)
PTL05	With GFRP tubes and elastic layers	✓	✓ (05 GPa)
PTL10		✓	✓ (10 GPa)
PTL15		✓	✓ (15 GPa)

Table 1: PPS specimens with different configurations of GFRP tubes and elastic layers.

Figure 1 compares all the PPS pier specimens considered in this study. A 3D FE modelling of the PPS pier is developed in ABAQUS [13]. Figure 2 shows geometric details of the PPS piers. The 3D FE model of the piers is defined with n segments (n = 6), of width B (B = 0.5 m) and height h (h = 0.5 m). To provide the self-centering mechanism under a lateral cyclic loading, an unbounded post-tensioned tendon passes through a duct in the segments, and is fixed to the top of the pier and the bottom of the foundation. The duct has a diameter of 80 mm, and the post-tensioned tendon area is considered 20 % of the segment area [14]. The elastic layers of height of h_L (h_L = 5 cm) are used between the segments.

The segments, foundation, and tendon are modelled using eight-node 3D brick elements (C3D8R). The segments, layers, and tendons are deformable solids while the foundation is a discrete rigid element. The GFRP tubes are modelled as shell elements around the concrete segments. To model the joints, the surface-to-surface contact elements are adopted. The tangential friction between the surfaces is taken 0.5 [15]. To model the normal contact between the surfaces, the hard contact is used. To model the unboundedness of the tendon, the frictionless surface-to-surface contact element is adopted between the tendon and the inside face of the ducts, through the segments and layers. The unbounded tendon is embedded in a load stub at the top of the pier and in the foundation.

Figure 1: The FE models of: (a) P, without GFRP tubes and elastic layer, (b) PT, with GFRP tubes, (c) PL, with elastic layers, and (d) PTL, with GFRP tubes and elastic layers.

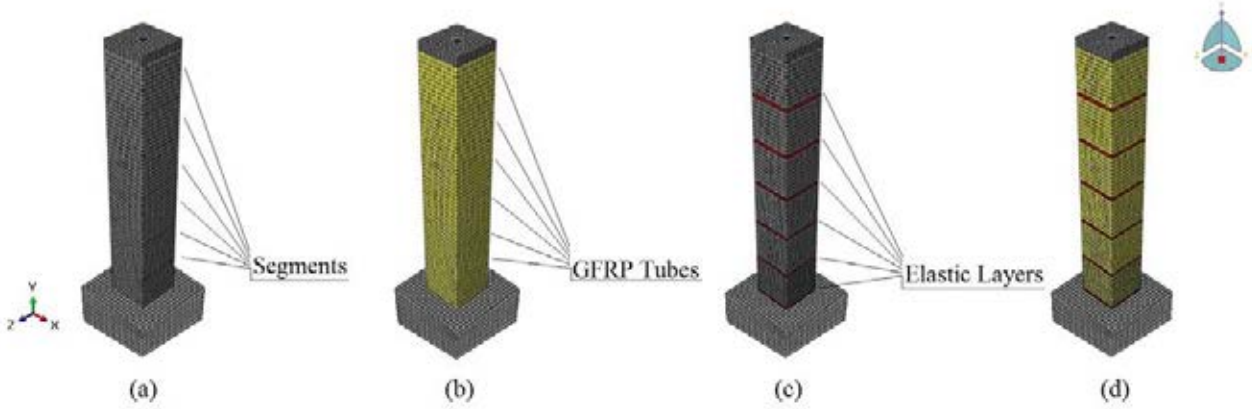

Figure 2: Geometric details of the piers: (a) P and PT, and (b) PL, and PTL.

To define concrete material of the segments, there are two models in ABAQUS: (*i*) smeared cracking model, and (*ii*) damaged plasticity model. The concrete damage plasticity is recommended for concrete piers subject to monotonic, cyclic and dynamic loading as used in this study [13,16]. Figure 3a shows the stress-strain of concrete for both confined (with GFRP tubes) and unconfined (without GFRP tubes) concrete [17]. The concrete's modulus of elasticity, Poisson's ratio, and density are 34.6 GPa. 0.2, and 22 kN/m^3, respectively. To simulate the opening between the joints, tension strength of concrete is taken zero. The post-tensioning tendon is modelled by a bilinear elastic-plastic model, shown in Figure 3b. The initial post-tensioning of the tendon is $T_0 = \alpha f_y$, where α is the yield force ratio of the tendon, 0.2, and f_y is yield stress of the tendon. The tendon's modulus of elasticity, yielding stress, Poisson's ratio, and density, 200 GPa, 2000 MPa, 0.3, and 78.4 kN/m^3, respectively. To model the GFRP tubes, the elastic behavior of Lamina type is used [13]. To develop the material properties, five constants are required: three shear moduli ($G12$; $G13$; $G23$) and two Young's moduli

($E11$; $E22$). Each shear modulus is taken 3 MN/m^2, and each Young's modulus is considered 65 GN/m^2.

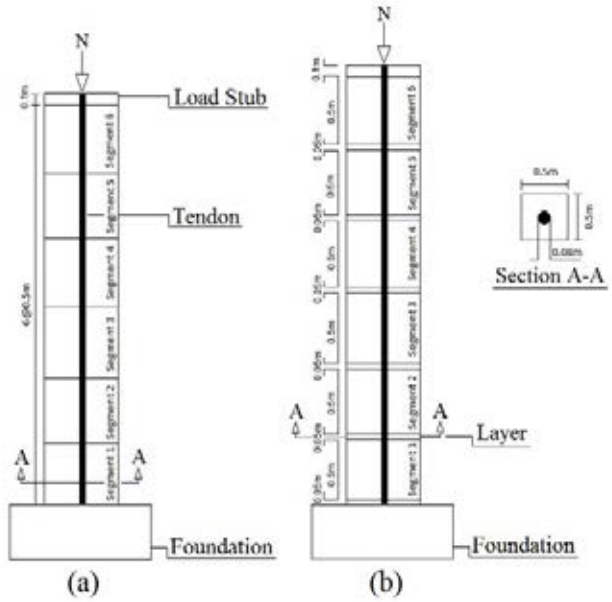

Figure 3: Stress-Strain models of: (a) concrete, and (b) steel.

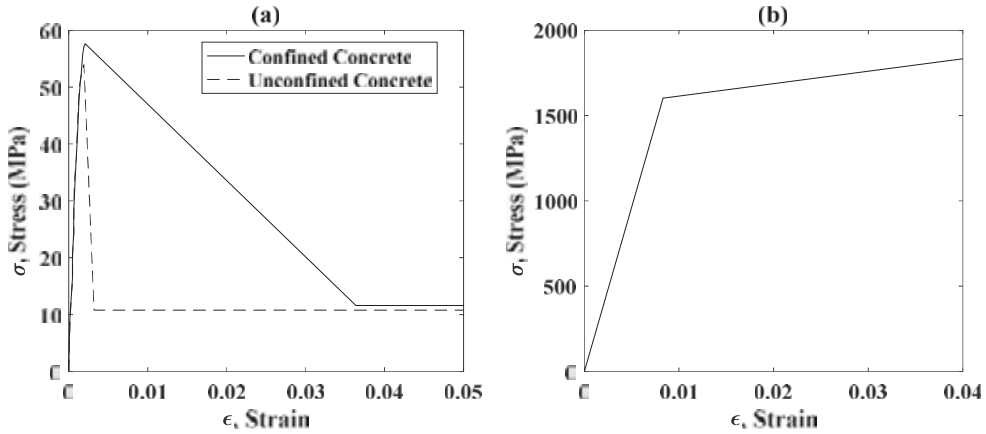

The axial load subject to the pier is a fraction of the axial capacity of the concrete section, $N = \beta f_c' A_g$, where β is axial load ratio, 0.2; f_c' is compressive strength of concrete, and A_g is the segment area. A gravity analysis is performed first, followed by a cyclic analysis. Displacement-control method is used to apply a cyclic loading pattern to the control node located at the top node of the topmost segment. Figure 4 shows the cyclic loading pattern considered.

Figure 4: Cyclic loading pattern.

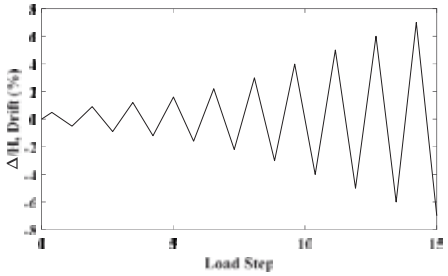

3 VALIDATION

The modelling approach, explained in Section 2, is validated through comparing with the experimental results by Palermo et al. [16,18]. The tested pier is composed of one concrete segment of height 1.6 m, and width 0.35 cm without any elastic layer or GFRP tubes. The model has two φ12.7 mm tendons, which pass through a pair of ducts in the segment and are fixed to a load stub at the top of the pier and a foundation at the bottom of the pier, as shown in Figure 5. The post-tensioning force ratio, α, is 0.3, and the compressive strength of concrete, f_c', is 54.1 MPa. The yield stress, f_y, and ultimate stress, f_u, of the post-tensioned tendons are assumed 1600 MPa and 1870 MPa, respectively. All the details of the modelling and loading are the same with those in the Palermo's test [16]. As Figure 6 shows, the lateral force-drift of the FE model and the test are very compatible, which demonstrates the robustness of the FE model in capturing lateral behavior of post-tensioned rocking piers. This comparison validates the reliable simulating of the models to study the behavior of the PPS piers.

Figure 5: Geometric details of the tested pier.

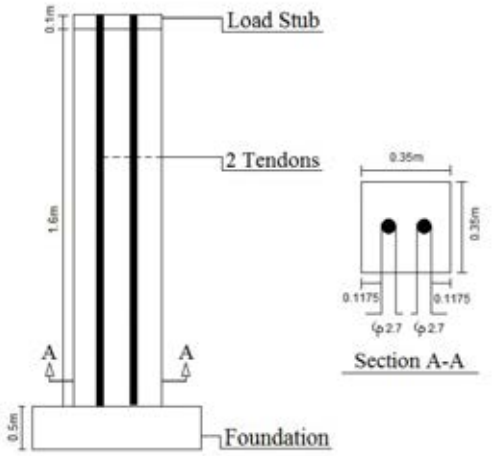

Figure 6: Comparison of FE modelling and test pushover curves.

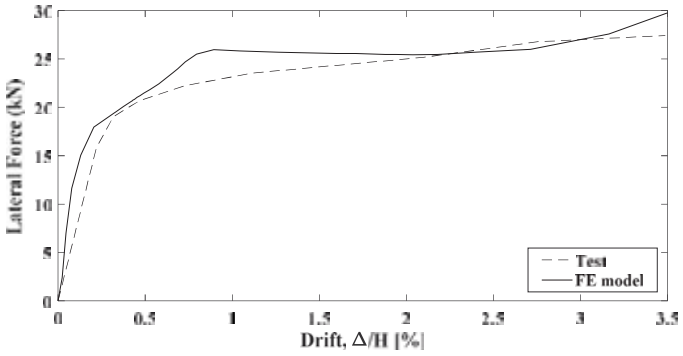

4 ANALYSIS AND RESULT

In this section, the cyclic behaviors of the eight piers, summarized in Table 1, are compared. Figure 7 demonstrates hysteretic response curves of the piers: the base shear, V, versus drift, Δ/H ; Δ is the tip displacement of the pier, and H is the total height of the pier. The results demonstrate different cyclic behavior for each pier. The pier, P, without any tube and layer, demonstrates a sudden reduction in its stiffness as the slope of the hysteretic loops suddenly drops after a few cycles at small drift ratios, less than 1% (Figure 7a). This stiffness re-

duction is due to the concrete spalling and crushing at small drift ratios at the toe of the segments (see Figure 3a). Adding GFRP tubes around the pier's segment, enhances the strength and slightly the ductility of the pier (Figure 7b). However, significant residual drifts are seen, particularly for the last cycles of the loading. Adding elastic layers between the segments slightly affects the strength of the pier, and gives zero-residual drift for the pier (Figure 7c). The simultaneous use of elastic layers and GFRP tubes increases ultimate strength of the pier, and results in zero-residual drift. This is very desirable in a PPS pier as it is intended to be a damage-free pier (zero-residual drifts).

Figure 7: Hysteretic response curves of the piers: (a) P, (b) PT, (c) PL15, and (d) PTL15.

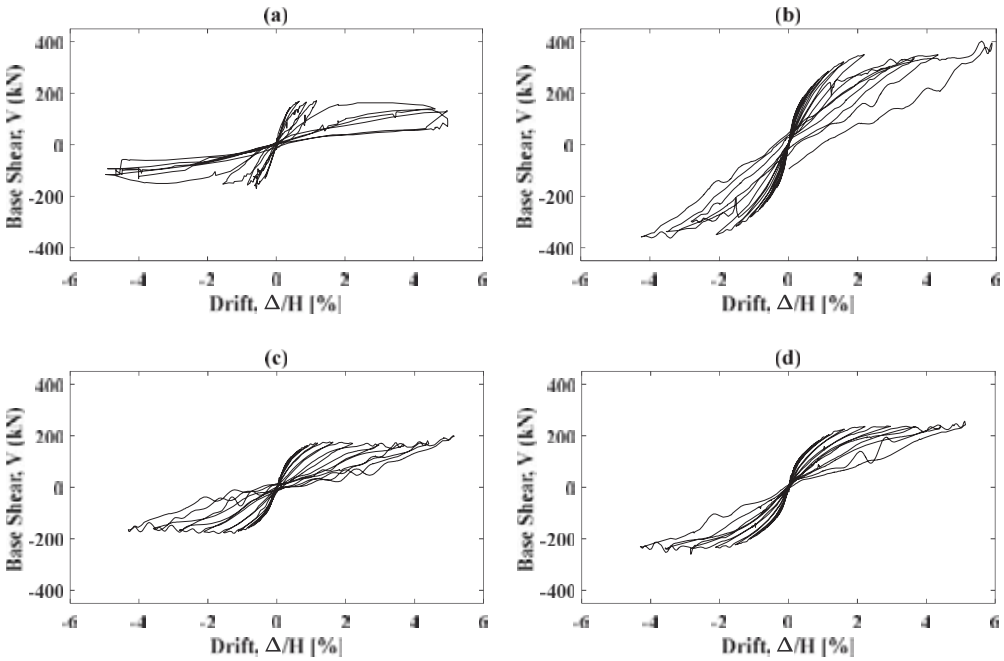

Figure 8 shows hysteretic response curves of the piers with different values of Young's modulus for the elastic layer. It is seen that the models with both GFRP tubes and elastic layers reach higher lateral strength. For the piers, PL and PTL, (Figures 8a and 8b), larger Young's modulus of the elastic layers gives higher lateral strength; The maximum value of base shear for Young's modulus of 15 GPa are 200 and 273.8 kN, for the piers PL and PTL, respectively.

Figure 8: The effect of Young's modulus of the layer on the hysteretic response curves of the piers: (a) PL, and (b) PTL.

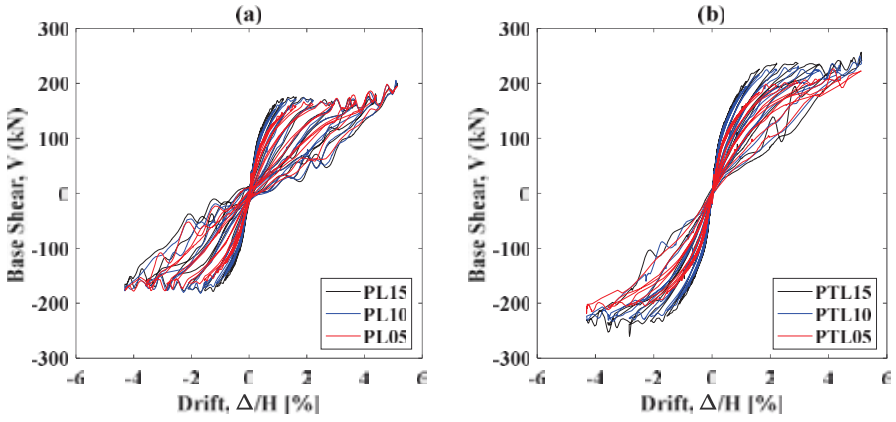

Figure 9 shows the stress at the toe of the bottommost joint (base joint), located between the bottom segment and the foundation, for the piers P, PT, PL15, and PTL15. For the pier P, after a few cycles of loading, the concrete crushes at the toe subject to high value of strain (see Figure 3a), and consequently, an abrupt drop is seen in the compressive stress at very small drifts, less than 1% (Figure 9a). Using GFRP tubes around the segments delays the stress drop by adding confinement to the concrete (Figure 9b). Adding elastic layers to the pier eliminates the sudden drop in the compressive strength of concrete (Figure 9c). The pier with both GFRP tubes and elastic layers (Figure 9d) reaches to higher compressive strength for higher values of drift compared to when using elastic layers only (Figure 9c). Figures 10 and 11 show the stress at the topmost, second bottom, and bottommost joints of the piers, PL and PLT. For both piers, the bottommost joint experiences the highest stress and local damage at their toes. The maximum values of stress is obtained for the models with Young's modulus of 15 GPa (PL15 and PTL15).

Figure 9: Compressive stress at the toe of the bottommost joint for the piers: (a) P, (b) PT, (c) PL15, and (d) PTL15.

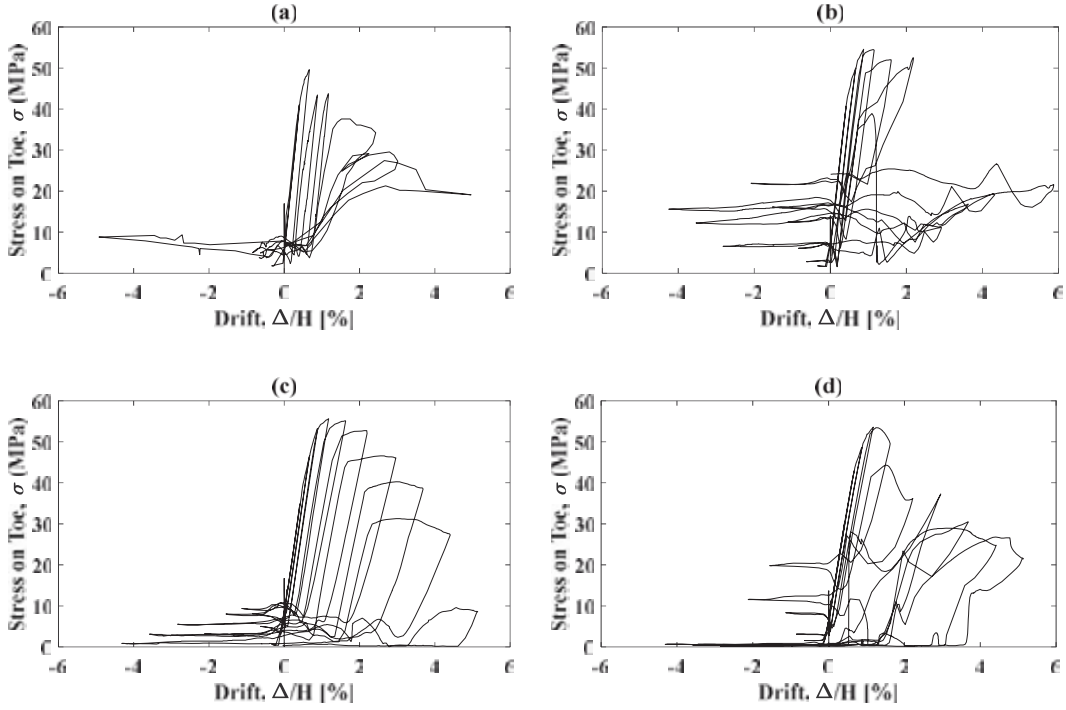

Figure 10: The effect of Young's modulus of the layer on the stress at: (a) the topmost joint, (b) the second bottom joint, and (c) the bottommost joint of the pier PL.

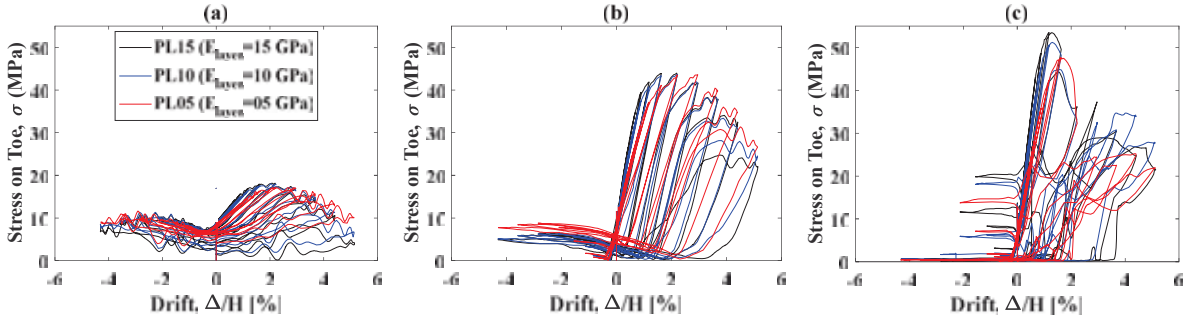

Figure 11: The effect of Young's modulus of the layer on the stress at: (a) the topmost joint, (b) the second bottom joint, and (c) the bottommost joint of the pier PLT.

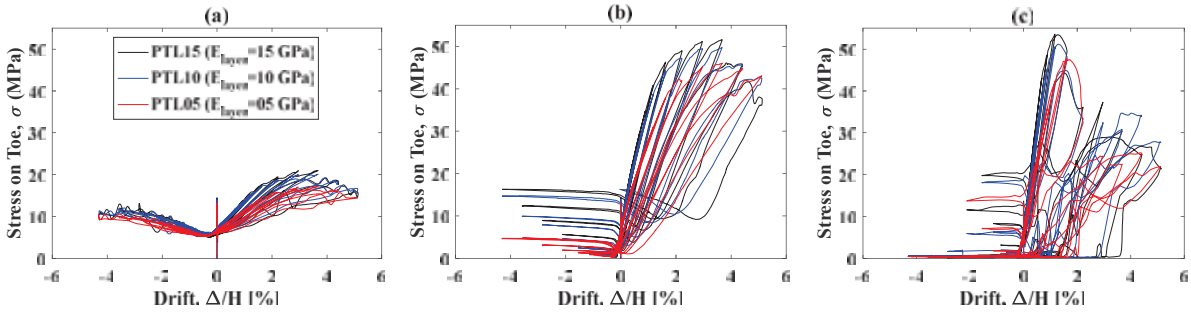

5 CONCLUSIONS

In this study, the effects of GFRP tubes and elastic layers on local damage of PPS piers were investigated. Hence, an FE model including GFRP tubes around segments and elastic layers in joints between segments were modelled using ABAQUS software.

It is found that elastic layers significantly reduce local damages at the joints, and GFRP tubes improve the results for large drifts. The results also show that GFRP tubes increase strength of the PPS piers, and both elastic layers and GFRP tubes give a zero-residual drift for the pier. These conclusions are very promising in designing a damage-free PPS pier. Hence, elastic layers need to be designed, and experimental tests need to be conducted for further investigation and validation of the proposed strategy.

REFERENCES

[1] M. Tazarv, M. Saiid Saiidi. Low-damage precast columns for accelerated bridge construction in high seismic zones. *Journal of Bridge Engineering*, **21(3)**, 04015056, 2016 Mar 1.

[2] H. Dawood, M. ElGawady, J. Hewes, Behavior of segmental precast posttensioned bridge piers under lateral loads. *Journal of Bridge Engineering,* **17(5)**, 735-46 ,2012 Sep 1.

[3] SL. Billington, RW. Barnes, JE. Breen, A precast segmental substructure system for standard bridges. *PCI journal,* **44(4)**, 56-73, 1999 Jul 1.

[4] MA. ElGawady, A. Sha'lan, Seismic behavior of self-centering precast segmental bridge bents. *Journal of Bridge Engineering,* **16(3)**, 328-39, 2011 May 1.

[5] AA. Maghsoudi, R. Rahgozar, SH. Hashemi, Flexural testing of high strength reinforced concrete beams strengthened with CFRP sheets. *International Journal of Engineering,* **1, 22(2)**, 131-46, 2009 Aug.

[6] SA. Sheikh, SA. Jaffry, C. Cui, Investigation of glass-fibre-reinforced-polymer shells as formwork and reinforcement for concrete columns. *Canadian Journal of Civil Engineering,* **34(3)**, 389-402, 2007 Mar 1.

[7] KA. Soudki, MF. Green, Performance of CFRP retrofitted concrete columns at low temperatures. *In2nd International Conference on Advanced Composite Materials in Bridges and Structures*, Montreal, Quebec, 11-14, 1996 Aug 11.

[8] O. Youssf, MA. ElGawady, JE. Mills, X. Ma, Finite element modelling and dilation of FRP-confined concrete columns. *Engineering Structures,* **79**, 70-85, 2014 Nov 15.

[9] Hewes JT, Priestley MJN., Seismic design and performance of precast concrete segmental bridge columns. *Report no. SSRP-2001/25*, University of California, San Diego, 2002.

[10] M. ElGawady, AJ. Booker, HM. Dawood, Seismic behavior of posttensioned concrete-filled fiber tubes. Journal of Composites for Construction, **14(5)**, 616-28, 2010 Oct.

[11] MA. ElGawady, A. Sha'lan, Seismic behavior of self-centering precast segmental bridge bents. *Journal of Bridge Engineering,* **16(3)**, 328-39, 2011 May 1.

[12] CC. Chou, YC. Chen, Cyclic tests of post-tensioned precast CFT segmental bridge columns with unbonded strands. *Earthquake engineering & structural dynamics,* **35(2)**, 159-75, 2006 Feb.

[13] SL. Billington, JK. Yoon, Cyclic response of unbonded posttensioned precast columns with ductile fiber-reinforced concrete. *Journal of Bridge Engineering,* **9(4)**, 353-63, 2004 Jul.

[14] Simulia DS. Abaqus 2017, Documentation. Providence, Rhode Island, US, 2017.

[15] E. Ahmadi, MM. Kashani, Numerical investigation of nonlinear static and dynamic behaviour of self-centring rocking segmental bridge piers. *Soil Dynamics and Earthquake Engineering,* **128**, 105876, 2020 Jan 1.

[16] H. Zhu, MT. Stephens, CW. Roeder, DE. Lehman, Inelastic response prediction of CFST columns and connections subjected to lateral loading. *J. Constr. Steel Res.,* **40,** 132:130, 2017,

[17] BD. Scott, R. Park, MJ. Priestley, Stress-strain behavior of concrete confined by overlapping hoops at low and high strain rates. *InJournal Proceedings,* **79.1**, 13-27, 1982 Jan 1.

[18] A. Palermo, S. Pampanin, D. Marriott, Design, modeling, and experimental response of seismic resistant bridge piers with posttensioned dissipating connections. *Journal of Structural Engineering,* **133.11**, 1648-61, 2007 Nov.